Excess of low-energy excitations in glasses

G. Carini, G. D'Angelo, and G. Tripodo
INFM, Dipartimento di Fisica, Università di Messina, Contrada Papardo Salita Sperone 31, 98166 S. Agata, Messina, Italy

A. Fontana and A. Leonardi
INFM, Dipartimento di Fisica, Università di Trento, 38050 Povo (Trento), Italy

G. A. Saunders
School of Physics, University of Bath, Claverton Down, Bath, United Kingdom

A. Brodin*
Department of Physics, Chalmers University of Technology, S-41296 Gothenburg, Sweden
(Received 26 April 1995)

Low-frequency Raman spectra of metaphosphate glasses $(Sm_2O_3)_x(P_2O_5)_{1-x}$, $(Eu_2O_3)_x(P_2O_5)_{1-x}$, $(Gd_2O_3)_x(P_2O_5)_{1-x}$, and GeO_2 have been measured in a wide temperature range from $T \approx 10$ K to the respective glass transition temperatures $T \approx 1000$ K. Analysis of the Raman data in comparison with complementary low-temperature specific heat, and ultrasonic measurements reveals that the temperature and frequency dependences of the quasielastic scattering and boson peak, as well as anomalous low-temperature specific heat, are in qualitative agreement with the predictions of soft potential model (SPM). In the case of the spectral density of "excess" soft modes, which are assumed to coexist and interact with ordinary phonons, the agreement can even be made quantitative under the restricted assumptions that the low-frequency Raman scattering reflects the *total* (phonon + excess) density of states, and the photon-vibration coupling constant is approximately linearly dependent upon frequency. However, neither of these assumptions are compatible with recent formulations of SPM.

I. INTRODUCTION

This work extends the initial report[1] in which Raman scattering, specific heat, and ultrasonic measurements on samarium phosphate glasses were used to test predictions of some recent theoretical models introduced to explain the dynamics of disordered systems and in particular the soft potential model (SPM). In order to test the general applicability of the model to very different glass systems, a wide ranging and detailed study of these properties has now been carried out in gadolinium and europium metaphosphate glasses and in vitreous germanium oxide.

Extensive research performed over the last two decades on different aspects of the glassy state has established a number of peculiar physical properties that are strikingly different from those of the respective crystalline solids[2] and are now being commonly referred to as universal for disordered systems. Some of these effects concern low-energy dynamics and manifest themselves in low-temperature specific heat, thermal conductivity, and inelastic scattering experiments. An important conceptual result of the low-energy behavior is that disordered systems support, in addition to the Debye-like phonons (nondispersive thermal plane waves), some other "excess" modes. The lowest-energy excitations (corresponding to $T \lesssim 1$ K) can be successfully described in terms of two-level systems (TLS's), or more generally tunneling systems (TS's), coexisting and interacting with Debye phonons. A nearly constant density of states of TLS's then provides a linear excess contribution to the specific heat, while phonon scattering from TLS's allows for adequate interpretations of heat conductivity, ultrasound attenuation, and dispersion experiments. However, at higher temperatures effects are observed which cannot be accounted for by this TLS model. Above 1 K the thermal conductivity reaches a plateau, while the specific heat exhibits further excess over that predicted by the standard Debye model, which is manifested in a bump in a C_p/T^3 vs T plot. The corresponding total density of vibrational states (DVS) $g(\omega)$, deduced from inelastic neutron scattering measurements, exhibits a broad maximum in a $g(\omega)/\omega^2$ vs ω plot, indicating again a non-Debye behavior. The excitations responsible have been proved to be essentially harmonic by a number of inelastic scattering and infrared absorption experiments, thus confirming that TLS's alone cannot account for the anomalous properties. In a number of models the enhancement of $g(\omega)$ in the frequency range $\gtrsim 10\,\mathrm{cm}^{-1}$ is explained by phonon localization due to strong scattering of phonons with wavelengths comparable to the length scale of static density fluctuations in the intermediate range (5–50 Å),[3] or to a regime of fractal dynamics (fractons) at higher frequencies.[4–6] Another possible approach (adopted in the SPM) is to assume that Debye-like phonons remain well-defined excitations in this frequency range, while "excess" vibrational states of dis-

tinctly different nature *coexist* with them, thus accounting for the excess in the specific heat and total density of vibrational states. This question of whether excess states and phonons can be considered as independent has implications in any interpretation of optical spectroscopic data. While low-temperature heat capacity and inelastic neutron scattering measurements yield rather unambiguous data for the total density of states, optical scattering and absorption spectra are affected by the *efficiency* of the photon-to-vibration coupling as well, and it is natural to expect different coupling coefficients for the excitations of different nature. In particular, first-order Raman scattering in a disordered system is conventionally expressed by the vibrational density of states $g(\omega)$ modulated by the coupling function $C(\omega)$:[7]

$$I^{\text{expt}}\omega/[n(\omega,T)+1] = C(\omega)g(\omega), \tag{1}$$

where $n(\omega,T)$ is the population factor for a harmonic oscillator. For localized modes the respective coupling coefficients are determined by the elasto-optical constants p. For propagating modes, instead, coherent scattering in the range of frequencies probed by Raman scattering is forbidden by the momentum transfer restrictions. The remaining incoherent scattering is then determined by fluctuations of the elasto-optical constants δp,[8] which are assumed to be small compared to the entire constant p. Consequently, if propagating modes (phonons) coexist with other localized modes of similar frequencies, then a Raman spectrum can be expected to reflect only a part of the density of states, corresponding to the localized excitations, rather than the total density of vibrational states. However, the available experimental data based on the direct comparison of Raman spectra with neutron scattering ones[9–12] and low-temperature heat capacity[13] strongly suggest that for a number of glasses Raman scattering spectra reflect the total DVS, with a smoothly varying coupling function $C(\omega)$ usually almost linear in frequency. A broad band observed in glasses in the range $20 - 100\,\text{cm}^{-1}$ — the boson peak (BP) — is then identified with the corresponding bump in the $g(\omega)/\omega^2$ frequency dependence.

At lower frequencies ($\lesssim 20\,\text{cm}^{-1}$) and elevated temperatures ($\gtrsim 20\,\text{K}$) Raman spectra of glasses show another characteristic feature, the quasielastic scattering (QS), which is usually attributed to some relaxational processes, as it is centered around zero frequency and increases in intensity with temperature at a higher rate than the Bose population factor. It is likely that the corresponding excitations are related to the TLS's. In fact, TLS's can couple to light scattering directly, as was originally indicated by Jäckle.[8] However, a more probable mechanism must involve indirect coupling via mechanical coupling to phonons;[8] this follows from the fact that the depolarization ratio is always the same for QS and BP. The microscopic origin of QS should then be the same as that which causes the acoustic attenuation peaks which occur above 20 K in glasses.[14–16] Application of this model has provided a successful interpretation of Raman scattering data in vitreous silica[8] and B_2O_3,[17] but was unable to describe quantitatively experimental results in other glasses.[18] Hence, TLS's alone cannot account for the experimental data; other mechanisms seem to contribute as well.

The universality of the low-temperature and low-frequency anomalies of the glass dynamics suggests that their different aspects may be interrelated and have the same microscopic origin. The only theoretical model introduced so far to account for a majority of these properties in a quite general way is the SPM. Originally proposed by Karpov, Klinger, and Ignatiev[19] and by Karpov and Parshin[20] and further developed in a number of works, (Refs. 21–23 and references therein), this model is intended to give a unitary description of the low-energy glass dynamics and may be considered as an extension of the TLS model to include and describe higher-energy excitations.

The present objective has been to test the applicability of the SPM to a number of glasses by means of Raman spectroscopy, calorimetry, and ultrasonic measurements. In the next section a brief description of the model and its main predictions pertinent to the data analysis and interpretation are given following standard SPM notation. Subsequent sections present experimental data and discussion, emphasizing controversial points and results which diverge from model predictions.

II. SOFT POTENTIAL MODEL

The SPM approach assumes that the low-frequency dynamics of glasses is characterized by the presence of strongly localized excitations, which coexist with ordinary sound waves (extended modes).[19,21–23] It is argued that, for the localized modes, anharmonicity of an effective local potential needs to be taken into account, as the average square displacements for localized modes must be relatively high. This is usually expressed as an expansion in power series of an appropriately chosen configurational coordinate x:

$$V(x) = \mathcal{E}[\eta(x/a)^2 + \xi(x/a)^3 + (x/a)^4], \tag{2}$$

where $\mathcal{E}$ is an energy of the order of 10 eV, a is a distance of the order of interatomic spacing, and η and ξ are small random parameters. The distribution function of η and ξ is written as

$$P(\eta,\xi) = P_0|\eta|, \tag{3}$$

where P_0 is usually taken as being constant. The lowest-energy excitations for the potential of Eq. (2) are two-level tunneling systems, while the distribution of Eq. (3) allows for the correct description of their density of states, which is well known to be nearly constant in energy. It is to be noted that in the energy range of the TLS the model adds nothing to the conventional picture. The crucial idea of the model is that the same mechanism of Eq. (2) determines the next-higher-energy excess excitations, which appear as quasiharmonic oscillators (HO's). They interact with acoustic phonons in the same way as TLS's do, the interaction being either resonant or

nonresonant ("relaxation"). The result of this interaction is expressed through the inverse phonon mean free path, which is determined by the resonant and nonresonant processes associated with both TLS's and HO's: $l^{-1} = l^{-1}_{\mathrm{rel,TLS}} + l^{-1}_{\mathrm{res,TLS}} + l^{-1}_{\mathrm{rel,HO}} + l^{-1}_{\mathrm{res,HO}}$. In the potential written as Eq. (2), TLS's exist up to a certain energy W (usually of the order of a few cm^{-1}), which marks a crossover to a different type of localized excitations — the HO's. For energies $\lesssim W$, the description of the interaction with phonons resembles the conventional one, as mentioned. At higher frequencies, the main mechanism of phonon scattering is resonant interaction with HO's, the respective contribution to l^{-1} being independent of temperature and proportional to the density of states of the HO's. So we have

$$N_{\mathrm{HO}} = \frac{1}{3\sqrt{2}} \frac{P_0 \eta_L^{5/2}}{W} \left(\frac{\hbar\omega}{W}\right)^4 . \tag{4}$$

An ω^4 dependence of Eq. (4) for the excess DVS above W is an important prediction of the SPM which is to be checked experimentally. In particular, it yields a T^5 excess heat capacity above a few kelvin (by "excess" we mean, throughout the paper, an excess over the Debye contribution). A crossover from a linear specific heat of TLS's at lower temperatures to a T^5 dependence of HO's then determines the characteristic energy W. The SPM introduces another characteristic energy E_d=(0.6–0.75)$WC'^{-1/3}$, C' being a dimensionless parameter (for its definition see Sec. III C), which sets the high-energy limit of the HO description and is usually identified with the maximum of the BP, and hence is of the order of $\omega_d \sim 30$–$50\,\mathrm{cm}^{-1}$. The excitations above E_d are thought to be neither localized soft modes nor phonons, but rather new delocalized states resulting from an ensemble of strongly interacting soft modes. An estimate of the reconstructed DVS is obtained as

$$\tilde{N}(\omega) \propto \omega, \quad \omega > \omega_d. \tag{5}$$

Within the SPM Raman scattering from the soft potentials is treated, following the standard theory for light scattering, and is expressed through the phonon mean free path, making use of the fluctuation-dissipation theorem[22]

$$I(\omega, T) \propto ([n(\omega, T) + 1]/\omega) l^{-1}(\omega, T), \tag{6}$$

where l^{-1} is the inverse mean free path of acoustic phonons. It is then assumed[21,22] that phonon attenuation and Raman scattering are both caused by time fluctuations of the same degree of freedom (generalized coordinate of a soft mode), as the latter cause a fluctuating elastic strain which is assumed to be linearly coupled to the strain associated with phonons (resulting in phonon attenuation), and to the electronic susceptibility via the elasto-optical constants (resulting in Raman scattering). It is further assumed that phonon spectral density as such is not "visible" in Raman scattering, for the reasons mentioned introduced with Eq. (1), or due to stated relative smallness.[21] It is also assumed that both soft mode configuration and effective mass are only weakly dependent on the respective eigenfrequency, so that these dependences can be neglected when evaluating the quantities like elastic strain associated with a mode and mode polarizability. This rather strong assumption has an important consequence, namely, that the coupling function $C(\omega)$ [see Eq. (1)] and the depolarization ratio of the low-frequency Raman scattering *do not* depend on frequency.

To summarize the SPM results on the phonon–soft-mode interaction, we present, without a discussion, different contributions to the phonon mean free path l^{-1}, which are of relevance for the present study:

$$l^{-1}_{\mathrm{res,HO}} = \frac{\pi}{6\sqrt{2}} \frac{C'\omega}{v} \left(\frac{\hbar\omega}{W}\right)^3 , \tag{7}$$

$$l^{-1}_{\mathrm{rel,TLS}} = \frac{\pi\omega C'}{v} \left(\frac{k_B T}{W}\right)^{3/4} \ln^{-1/4} \frac{1}{\omega\tau_0} , \tag{8}$$

$$l^{-1}_{\mathrm{rel,HO}} = \frac{16\pi}{9} \frac{C'\omega}{v} \frac{k_B T}{E_c} \left(\frac{W}{\hbar\omega}\right)^{1/2} . \tag{9}$$

III. EXPERIMENTAL TECHNIQUES

Rare earth metaphosphate glasses were prepared by melting well-mixed high purity oxides in an alumina crucible; detailed procedure has been described elsewhere.[24] Vitreous GeO_2 was made by melting high purity oxide in a platinum crucible. Each glass was of high optical quality. The compositions of the phosphate glasses were determined by electron probe microanalysis using SmS, $GdAl_2$ or EuS crystal as a standard. X-ray diffraction was used to make sure that the samples were purely amorphous. The surfaces were polished to optical quality in order to minimize the elastically scattered light which could have masked the low-frequency scattering.

Raman scattering measurements were performed in a helium cryostat for low temperatures and in an oven for high temperatures. The light source was an Ar^+ ion laser operating below 100 mW of the 514 nm line to avoid undue sample heating. The 90° scattered light was analyzed by a double pass grating monocromator, spectral slit width being set to $2\,\mathrm{cm}^{-1}$ throughout the measurements. All the measurements were carried out in both HV (depolarized) and VV (polarized) configurations.

The specific heat was measured using an automated calorimeter[25] which was operated by the relaxation method, using a silicon chip as a sample holder. The experimental error in the measured specific heat has been evaluated as about 3%. The attenuation and velocity of longitudinal and shear ultrasound waves were measured using conventional ultrasonic techniques in the 10–90 MHz frequency range and in the temperature interval 1.5–400 K.

IV. RESULTS

A. Raman spectra

The low-frequency Raman spectra of metaphosphate glasses $(R_2O_3)_x(P_2O_5)_{1-x}$, where $R = Eu^{3+}$, Gd^{3+}, or Sm^{3+}, and of GeO_2 glass have been measured, over a wide temperature range from $\sim$10 K up to the respective glass transitions temperatures T_g. The frequency range probed was extended up to 2000 cm^{-1}, with the low-frequency limit being 5–10 cm^{-1}, where a contribution from the instrumental tail is still negligible. In the present paper we limit ourselves to the analysis of the low-frequency ($\lesssim 50\,cm^{-1}$) behavior only, the higher frequency results being the subject of a separate paper.[26] We note that the depolarization ratio of a low-frequency spectrum is essentially independent of frequency and temperature, being of the order of 0.5–0.7 for different samples. Thus, the well-known fact of the same depolarization ratio of both the QS and BP (Ref. 8) is confirmed for the present systems. This property serves also as a convenient test of the data reliability at the low-frequency limit: The data are considered reliable down to that frequency where the depolarization ratio is still unchanged (elastically scattered central line, as well as its instrumental tail, are always polarized). Only depolarized (HV) Raman spectra will be considered from here on.

The depolarized (HV) low-frequency Raman spectra of some of the samples at selected temperatures are shown in Fig. 1. The spectra are presented in the spectral function (normalized) form $I_{expt}/[\omega(n+1)]$ vs ω, so that population factor temperature dependence is removed. The spectral region of BP above 25–30 cm^{-1} has an essentially harmonic (temperature-independent) behavior, up to the highest temperature used. The QS, which dominates the spectra at lower frequencies and elevated temperature, exhibits much stronger a temperature dependence than that of harmonic oscillators.

Now, the QS temperature dependence and spectral shape are analyzed. The QS can be extracted from Raman spectra measured at different temperatures, because the vibrational contribution follows the known temperature dependence of Bose factor. Thus, subtraction of Bose-corrected spectra at different temperatures removes the vibrational (harmonic) contribution and yields an "excess" — the QS:[18]

$$I_{QS}(\omega,T) = \left(\frac{I_{expt}(\omega,T)}{n(\omega,T)+1} - a\,\frac{I_{expt}(\omega,T_0)}{n(\omega,T_0)+1} \right) [n(\omega,T)+1]. \qquad (10)$$

Here $a \approx 1$ is a correction factor used to normalize the spectra above 40–50 cm^{-1} and thus accounts for minor variations in the measuring conditions at different temperatures. T_0 is the lowest measured temperature. The QS obtained in this way for $(Gd_2O_3)_{0.226}(P_2O_5)_{0.774}$ and GeO_2 samples at selected temperatures is presented in Fig. 2. The results for other samples and different temperatures are qualitatively the same. The QS intensity decreases with frequency and becomes vanishingly small above 40 cm^{-1}. Another important result is that, within the limits of experimental errors, the spectral shape of the QS *does not depend on temperature*. The same result has been reported previously for samarium phosphate glasses of different composition;[18] here it is confirmed for the glasses of present study. A consequence of this property is that the temperature behavior of the integrated intensity of the QS is identical to that taken at any frequency below 40 cm^{-1}, and in particular at the lowest frequency probed, where the respective vibrational contribution is relatively small at elevated temperatures. The results obtained for the QS temperature dependence, evaluated as

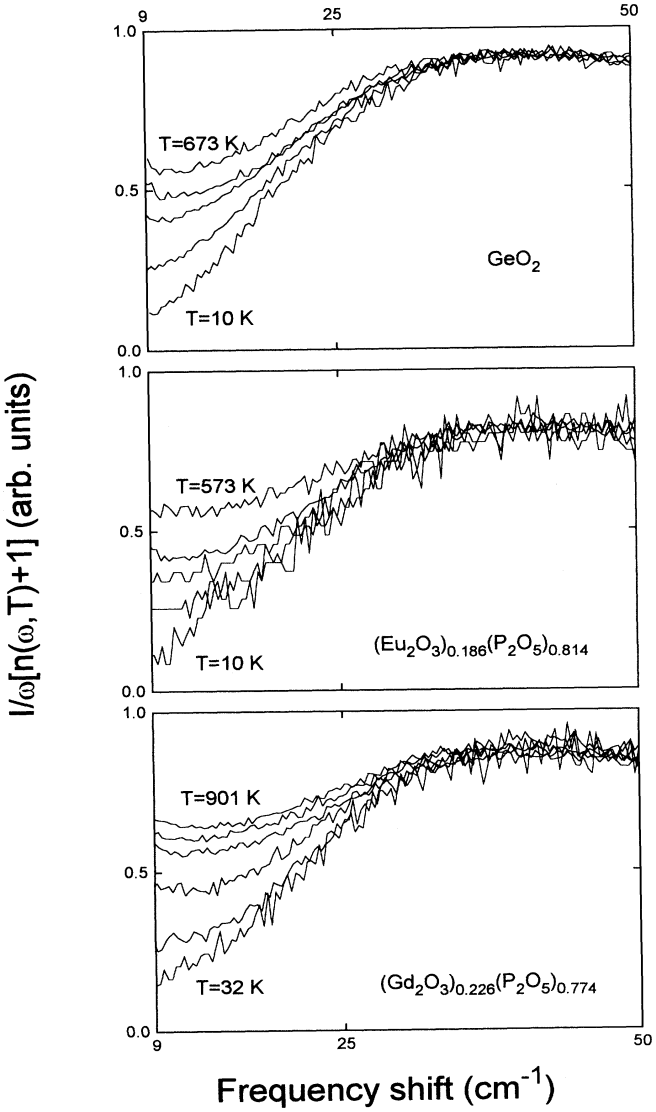

FIG. 1. Low-frequency Raman spectra $I/[\omega(n(\omega,T)+1)]$ of GeO_2, $(Eu_2O_3)_{0.186}(P_2O_5)_{0.814}$ and $(Gd_2O_3)_{0.226}(P_2O_5)_{0.774}$ glasses at selected temperatures, as indicated.

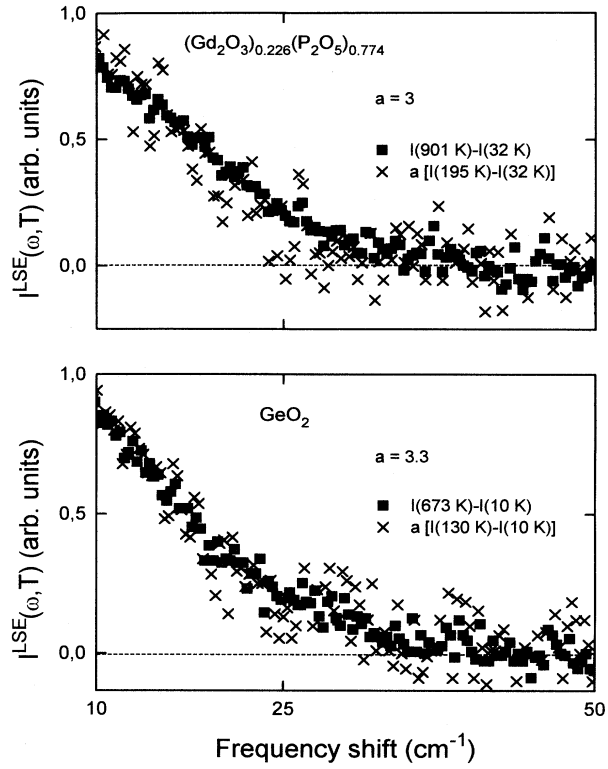

FIG. 2. Quasielastic part of Raman spectra at selected temperatures, deduced from measured spectra in Fig. 1 by removing the respective harmonic contributions, as discussed in the text.

the measured intensity at 8–10 cm^{-1}, are shown in Fig. 3. The temperature variation of $I_{QS}(T)$ may be approximated by a power law T^{β} for each glass, over the whole temperature range studied. The temperature exponents β are found to be material dependent and vary from 1.4 to 2.4 . Such a behavior, although material dependent, is close to what one expects for the relaxational contribution $\propto T^{1.75}$ associated with the TLS's [Eqs. (6),(8)] and the contribution $\propto T^2$ of the HO's [Eqs. (6),(9)].

Having analyzed the frequency and temperature dependences of the QS at elevated temperatures, we next examine the vibrational contribution of the BP. The lowest-temperature spectra are considered, as at low enough temperatures all relaxational mechanisms, determining the QS, are suppressed. Figure 4 shows low-temperature Raman spectra for a selection of samples, taken at 10–11 K and presented in a temperature-reduced $I_{expt}\omega/[n(\omega,T)+1]$ vs ω plot. The temperature of 10 K is low enough to suppress the QS: Extrapolation of the data of Fig. 3 down to 10 K yields negligible values compared to the measured intensities of Fig. 4. For frequencies below 30 cm^{-1} the data follow power law dependences (straight lines) with frequency exponents ranging from 3.5 to 3.8 (see Fig. 4). These frequency dependences are similar to those found in Se, As_2S_3, B_2O_3, and SiO_2 glasses,[13] and thus appear to be universal for a variety of glasses. The SPM predicts a dependence of ω^4, which resembles the one for the HO density of states [Eq. (4)] and is similar to those observed experimentally.

B. Specific heat results

The experimental specific heat results obtained between 1.5 K and 30 K for $(Eu_2O_3)_{0.186}(P_2O_5)_{0.814}$ and $(Gd_2O_3)_{0.226}(P_2O_5)_{0.774}$ glasses are shown in Fig. 5. The minimum found in the specific heat of $(Gd_2O_3)_{0.226}(P_2O_5)_{0.774}$ at about 5 K marks the onset of an increasing magnetic contribution to $C(T)$ at lower temperatures.[25] In fact, in glasses containing

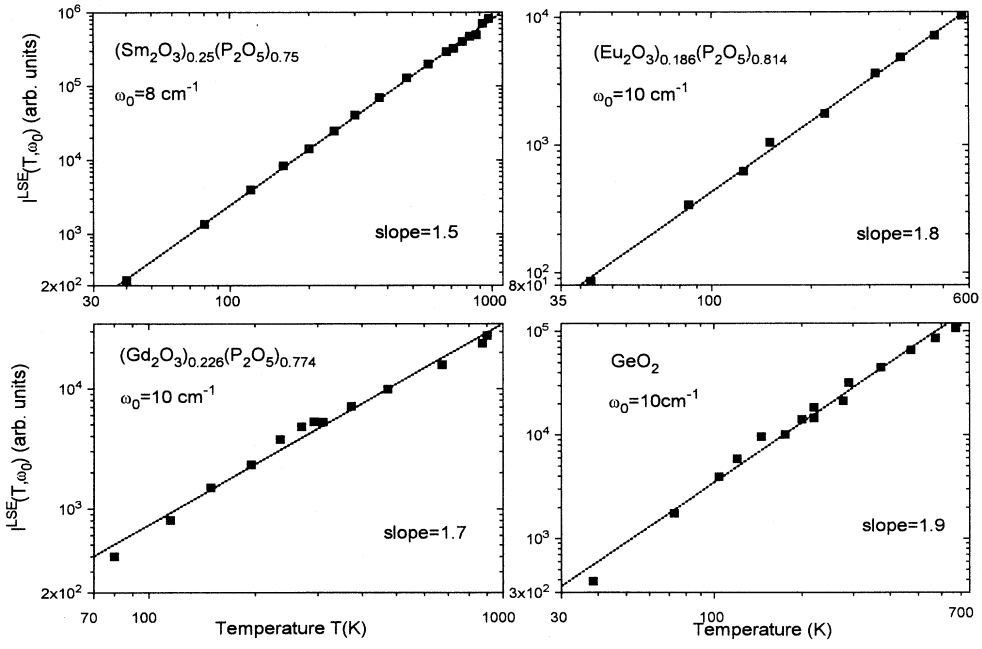

FIG. 3. Log-log plot of QS scattering intensity versus temperature, deduced from measured spectra in Fig. 1 as the intensity around ω_0. Points represent experimental data; lines are power law fits.

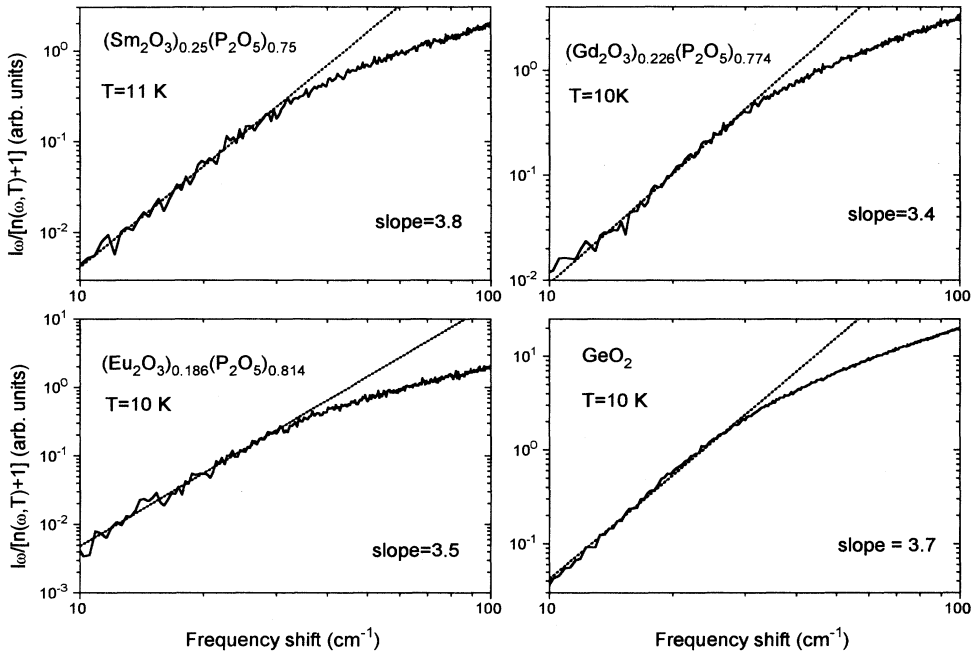

FIG. 4. Low-temperature Raman spectra in log-log plots. Lines are power law fits.

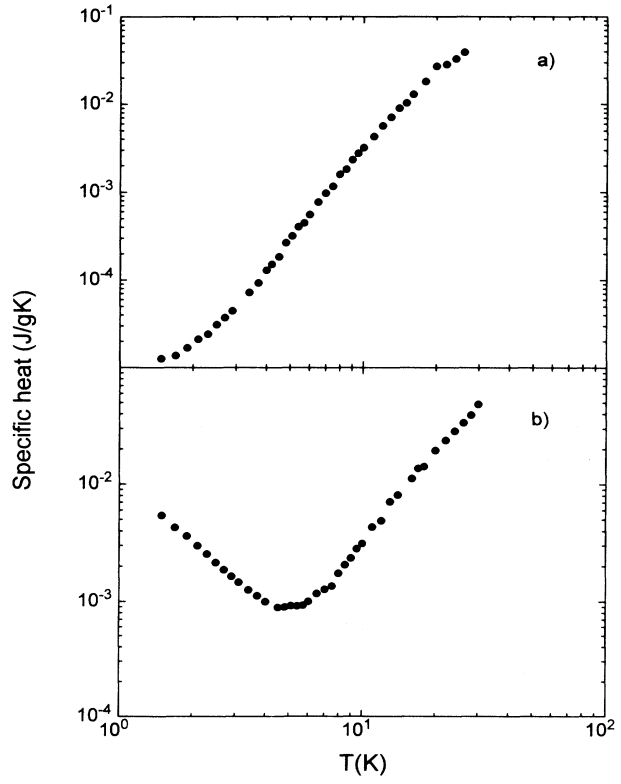

FIG. 5. Temperature dependences of the specific heat C for $(Eu_2O_3)_{0.186}(P_2O_5)_{0.814}$ (a) and $(Gd_2O_3)_{0.226}(P_2O_5)_{0.774}$ (b) glasses between 1.5 K and 30 K.

high concentrations of strongly paramagnetic Gd^{3+} ions, an enormous magnetic effect of the tail of the Shottky contribution ($C_{\rm mag} \propto T^{-2}$) dominates the specific heat and makes it impossible to estimate the vibrational contribution accurately.[25] By contrast, a small paramagnetic contribution influences the specific heat of $(Eu_2O_3)_{0.186}(P_2O_5)_{0.814}$ only below 3 K; this magnetic contribution has been separated off by a comparison with the specific heat data determined for the diamagnetic lanthanum metaphosphate glass having the same composition (see the inset of Fig. 6). Furthermore, it has established that the two glasses have the same vibrational specific heat down to $\approx$3 K. Using the experimental data of the lanthanum glass as a reference, it was possible to deduce the vibrational contribution for $(Eu_2O_3)_{0.186}(P_2O_5)_{0.814}$ which, if plotted as $[C(T) - C_{\rm Debye}]/T^3$ vs T (Fig. 6), exhibits a broad peak, characteristic for glasses, at about 10 K. The Debye contribution was computed from the experimental sound velocities (see Table I):

$$C_{\rm Debye} = \frac{2\pi^2 k_B^4}{5\hbar^3}\frac{T^3}{\rho \bar{v}^3} \quad ({\rm J\ g^{-1}\ K^{-1}}), \tag{11}$$

where $\bar{v} = [3(1/v_l^3 + 2/v_t^3)^{-1}]^{1/3}$ (cm s^{-1}) is the average sound velocity and ρ (g cm^{-3}) the mass density.

Within the SPM approach, the lowest-energy excitations are the usual TLS's with a nearly constant density of states. At temperatures ($T \ll W/k_B$) small compared with the energy W, which sets the crossover between the TLS and HO excitations, they contribute a linear term to the specific heat:[27]

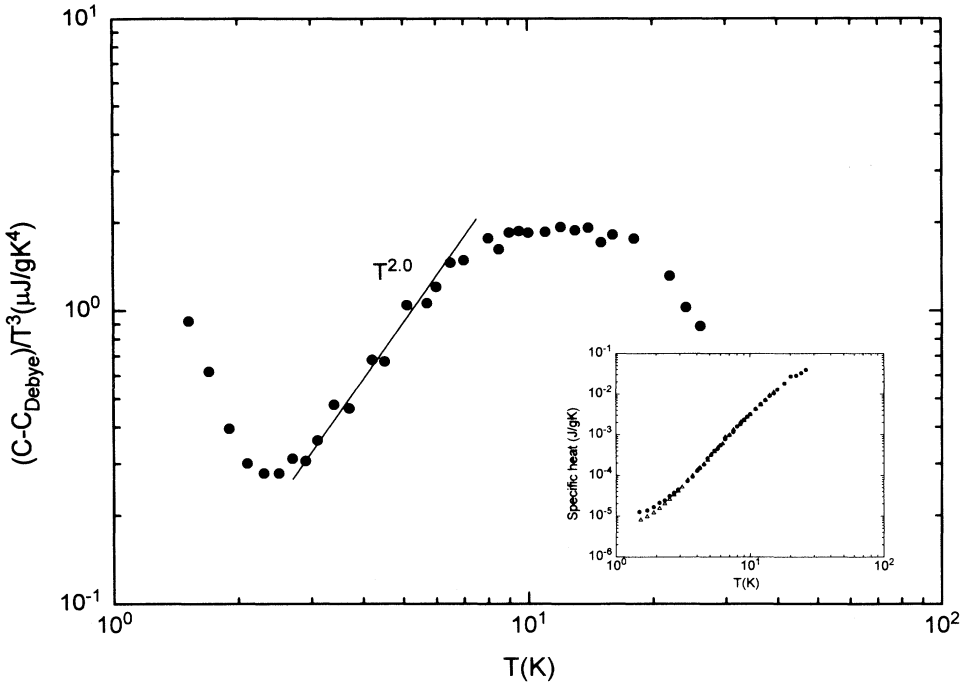

FIG. 6. "Excess" specific heat $(C - C_{\text{Debye}})/T^3$ versus temperature for $(Eu_2O_3)_{0.186}(P_2O_5)_{0.814}$. Inset: comparison of the specific heat data of the moderately magnetic $(Eu_2O_3)_{0.186}(P_2O_5)_{0.814}$ glass (•) and diamagnetic $(La_2O_3)_{0.19}(P_2O_5)_{0.81}$ glass (△).

$$C_{\text{TLS}}(T) = \pi^2 \left(\frac{2}{9}\right)^{1/3} \frac{P_0 \eta_L^{5/2}}{W} k_B^2 T \ln^{1/3} \times \left[\frac{W}{k_B T}\sqrt{\frac{t_{\text{expt}}}{\tau_{\min}(T)}}\right], \quad (12)$$

where the symbols are those defined in Ref. 27. At higher temperatures excitations with energies larger than W are responsible for the properties: When $T \gg W/k_B$, HO's are contributing to the specific heat, and their rapidly increasing density of states [see Eq. (4)] leads to a T^5 term in the latter:[27]

$$C_{\text{HO}}(T) = \frac{8\pi^6 k_B}{63\sqrt{2}} P_0 \eta_L^{5/2} \left(\frac{k_B T}{W}\right)^5. \quad (13)$$

At still higher temperatures, an ensemble of "collective," or delocalized, vibrational excitations is excited, and their linearity in frequency density of states [Eq. (5)] should correspond to a T^2 dependence of the specific heat. A crossover in the temperature dependence of the specific heat from the low-temperature linear dependence to a T^2 behavior through a T^5 dependence would lead to a minimum at certain $T_{\min}$ and maximum at $T \approx E_d/k_B$ in the temperature dependence of $C(T)/T^3$,[27] a behavior in accord qualitatively with that observed experimentally. $T_{\min}$ then determines the characteristic energy $W \sim 2k_B T_{\min}$. For the europium metaphosphate and germanium oxide glasses $T_{\min}$ appears to be 5 K and 4 K, respectively. For the europium metaphosphate glass this value, along with the value of C' deduced from ultrasonic data (see the following section and Table I), yields $E_d/k_B \approx 53$ K, which should be compared with the temperature of the maximum found at about 11 K.

Having established that the specific heat data are qualitatively in accord with the predictions of the SPM, we now turn to the quantitative analyses. As mentioned above, the SPM predicts three temperature regions with distinctly different behavior. For the specific heat expressed as $[C(T) - C_{\text{Debye}}]/T^3$ vs T these correspond to T^α dependences with different exponents α, varying from $\alpha_1 = -2$ for $T < T_{\min}$, through $\alpha_2 = 2$ for $T_{\min} < T < T_{\max} \approx E_d/5k_B$ to $\alpha_3 = -1$ at higher temperatures. The restricted temperature range available in our measurements makes it impossible to analyze accurately the first and the third temperature regions, yet an onset of T^α dependences with negative α_1 and α_3 is clearly observed (see Fig. 6). In the intermediate temperature range we obtain $\alpha_2 \approx 2.0$ and ≈ 1.8 for europium phosphate and germanium oxide glasses, respectively.

C. Acoustic attenuation and sound velocity

The temperature dependences of the ultrasound attenuation measured over the range 10 – 300 K are presented in Fig. 7. Above 10 K the attenuation increases towards a broad maximum, observed previously in metaphosphate glasses modified with different rare earth ions,[24] the maximum being shifted to higher temperatures as the ultrasonic driving frequency is increased.

For the gadolinium metaphosphate glass the attenuation measurements were made for both longitudinal and shear ultrasonic waves to find out if the attenuation mechanism was different for different polarizations: Within the experimental error, the internal friction $Q^{-1}(= \alpha\lambda/\pi)$ for both the longitudinal and shear modes was the same.

The velocity of the 10 MHz longitudinal and shear sound decreases with increasing temperature all the way from 10 K up to 300 K for both $(Eu_2O_3)_{0.186}(P_2O_5)_{0.814}$

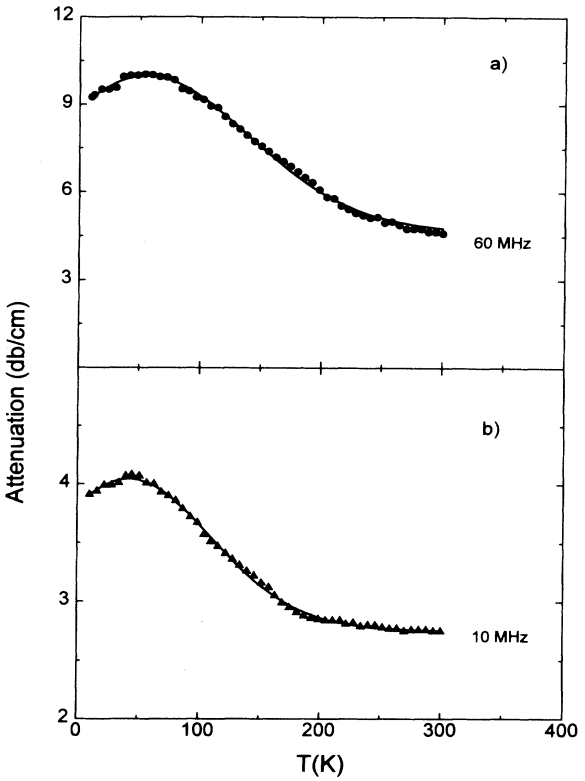

FIG. 7. Temperature dependences of the ultrasound attenuation of $(Eu_2O_3)_{0.186}(P_2O_5)_{0.814}$ (a) and $(Gd_2O_3)_{0.226}(P_2O_5)_{0.774}$ (b) glasses at selected frequencies. Solid lines represent the theoretical fits to the experimental data by Eq. (14).

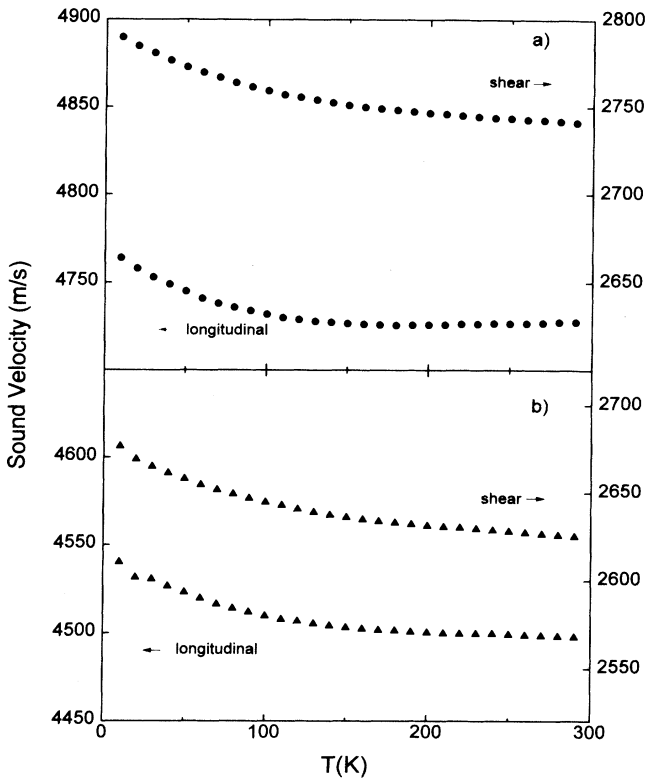

FIG. 8. Temperature dependences of the sound velocity of 10 MHz longitudinal and shear ultrasound in $(Eu_2O_3)_{0.186}(P_2O_5)_{0.814}$ (a) and $(Gd_2O_3)_{0.226}(P_2O_5)_{0.774}$ (b) glasses.

and $(Gd_2O_3)_{0.226}(P_2O_5)_{0.774}$ glasses; see Fig. 8. There is a trend characterized by a continuously changing slope below 100 K, which becomes nearly linear for higher T.

The relaxational attenuation has been analyzed, adopting the procedure elsewhere described[24] and based on the following expression:

$$\alpha_i = \frac{B_i^2}{4\rho v_i^3 k_B T} \int P(E) \frac{\omega^2 \tau(E)}{1+\omega^2\tau^2(E)}\, dE, \qquad (14)$$

where B_i is the average deformation potential that expresses the coupling between the ultrasonic stress and the system, v_i is the sound velocity, and τ is the relaxation time, which is assumed to follow Arrhenius-type behavior, $\tau^{-1} = \tau_0^{-1}\exp(-E/k_BT)$. $P(E)$ is a distribution function for N relaxing particles per unit volume and is taken as a Gaussian function with a most probable value E_m and a width E_0. The index i refers to the two different polarizations.

Using a single value of $\tau_0 = 10^{-14}$ s,[24] the values of E_m, E_0, and NB_i^2 have been obtained from the least-squares fits to the measured data. A typical fit of the relaxational losses is shown in Fig. 7 by a solid line, and the resulting relaxation parameters are given in Table I.

Now the relaxation parameters can be used to evaluate the magnitude of the excess contribution to the sound velocity due to the HO relaxation, which has been proved to be the dominant process below 100 K for this type of

TABLE I. Values of the parameters related to the thermal (E_m, E_0, and NB_l^2) and HO relaxation (C_l') in the glasses under study. Debye temperatures Θ_D were calculated from the longitudinal (v_l) and transverse (v_t) sound velocities and mass densities (ρ), measured at room temperature.

Sample	ρ (g cm^{-3})	v_l (m s^{-1})	v_t (m s^{-1})	Θ_D (K)	E_m (meV)	E_0 (meV)	NB_l^2 (10^{20} eV^2 cm^{-3})	C_l' (10^{-4})	W/k_B (K)
$(Sm_2O_3)_{0.25}(P_2O_5)_{0.75}$	3.52	4421	—	342	99	53	1.22	2.4	5
$(Eu_2O_3)_{0.186}(P_2O_5)_{0.814}$	3.182	4727	2741	376	62	91	2.43	2.92	5
$(Gd_2O_3)_{0.226}(P_2O_5)_{0.774}$	3.362	4498	2623	357	53	86	2.64	4.62	-
GeO_2[a]	3.629	3637	2233	293	-	-	-	-	4

[a]Data from Ref. 29.

metaphosphate glasses. The goal of this analysis is to deduce a complete set of parameters (thermal and acoustic) which, in the framework of the SPM model, allows for the temperature dependence of the QS to be reproduced.

The anharmonic contribution to the temperature dependence of the sound velocity has been estimated using the following equations:

$$v_l = v_{l0}\left(\frac{L}{L_0}\right)^{\frac{3}{2}}\left[1-\Gamma_l F\left(\frac{T}{\Theta}\right)\right]^{\frac{1}{2}} \tag{15}$$

with

$$F\left(\frac{T}{\Theta}\right) = 3\left(\frac{T}{\Theta}\right)^4 \int_0^{\frac{\Theta}{T}} \frac{x^3 dx}{e^x - 1},$$

where v_0 is the sound velocity in the limit $T \to 0$, L the length of the sample, Θ the Debye temperature, and Γ_l a coefficient depending, in particular, on the Gruneisen coefficient. Following the procedure described elsewhere,[24] the relative difference in velocity $\Delta v/v_0$ was evaluated. The calculated dependence of $\delta v/v_0$ for the $(Eu_2O_3)_{0.186}(P_2O_5)_{0.814}$ glass is shown in Fig. 9(a).

The dispersion arising from the thermally activated relaxation of the structural defects, which cause the peak of acoustic attenuation, has been evaluated by inserting the relaxation loss parameters in the following expression:

$$\left[\frac{\Delta v}{v_0}\right]_{\rm rel} = \frac{B_i^2}{8\rho v_i^2 k_B T}\int P(E)\frac{\omega^2\tau(E)}{1+\omega^2\tau^2(E)}\,dE. \tag{16}$$

The curve labeled "Rel" in Fig. 9(a) corresponds to the europium metaphosphate glass. The summed anharmonic and relaxation contributions underestimate the experimental effects, also shown for in Fig. 9(a) for the same glass, emphasizing the presence of a linear excess term in $\Delta v/v_0$ arising from the HO relaxation[24] obtained by taking differences of experimental values and those calculated by Eqs. (15) and (16), given in Fig. 9(a). This mechanism arises from the modulation of interlevel spacing by the sound wave and causes, in the ultrasonic range, a negligible attenuation and the following behavior of the sound velocity:[27]

$$\left[\frac{\Delta v}{v_0}\right]_{\rm HO} = -\frac{28\sqrt{2}}{9}C_i'\frac{k_B}{E_0}(T-T_0), \tag{17}$$

where $C_i' = P_0\gamma^2/\rho v^2$ is a dimensionless parameter defined by the spectral density of soft defects P_0 and the deformation potentials γ; $E_0 = 3W$ sets a crossover between the TLS and HO descriptions. The solid lines in Fig. 9(b) are a linear fit, as expressed by Eq. (17); the slopes then yield the values of C_i' for the two glasses (see Table I).

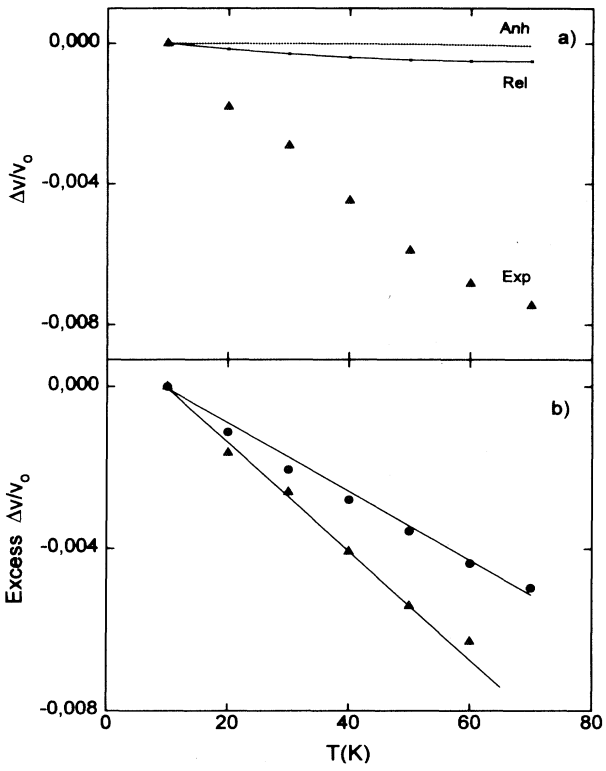

FIG. 9. (a) Comparison of the temperature dependences of the fractional sound velocity of 10 MHz longitudinal ultrasound in $(Eu_2O_3)_{0.226}(P_2O_5)_{0.774}$ glass with the anharmonic and relaxation contributions to $\Delta v/v_0$, calculated using Eqs. (16) and (17), respectively. (b) Excess contribution to the longitudinal sound velocity over that provided by anharmonic and relaxation processes of Eqs. (17) and (16) for $(Eu_2O_3)_{0.186}(P_2O_5)_{0.814}$ (•) and $(Gd_2O_3)_{0.226}(P_2O_5)_{0.774}$ (▲) glasses.

V. DISCUSSION

The data obtained by each of the experimental techniques used, correspond, qualitatively at least, to the respective SPM predictions. Now we can perform a more careful examination of the model applicability, based on a comparison of the results by different techniques used, as well as those found in the literature.

The relaxational and resonant processes of the SPM, associated with the TLS and HO, are directly accessible by Raman scattering and give rise to the QS and BP. An analysis of the spectral shape requires an assumption of the coupling function $C(\omega)$ [see Eq. (1)], while the temperature dependence of the QS does not depend on $C(\omega)$; so it is examined first. The relaxation contributions of TLS's [Eq. (8)] and HO's [Eq. (9)] yield $\propto T^{1.75}$ and $\propto T^2$ terms, respectively, in the QS Raman intensity [Eq. (6)], while the experimental temperature exponents are found to spread between 1.4 and 2.4 for different glasses. These values, although close to 1.75 and 2, cannot be quantitatively described by a combination of the contributing terms. Moreover, the experimental result of a temperature-independent spectral shape of the QS requires that only one of these terms be dominant, again irrespective of the choice of $C(\omega)$. Indeed, the TLS contribution to l^{-1} is $\propto T^{0.75}\omega$, while the one for HO's is $\propto T\sqrt{\omega}$, with the same Raman coupling coefficient for a given frequency. Consequently, the sum of these two contributions exhibits a temperature-dependent spectral

shape, unless one of the terms is negligibly small.

Concerning the evaluation of QS performed by acoustic and calorimetric data, using the SPM predictions, we emphasize that the theoretical fit is in reasonable agreement with the experimental data in samarium phosphate glasses,[28] but only qualitatively so for the gadolinium glass. This circumstance could arise from the fact that the magnetic contribution to the specific heat masks the vibrational one in the region where the minimum in C/T^3, which determines the crossover energy W, should be observed. Consequently for gadolinium glass the value of W obtained in a lanthanum glass with the same concentration has been used, hence assuming the same vibrational contribution for both the systems (see the inset in Fig. 6 as a reference).

Next we discuss the harmonic contribution to the Raman scattering. As we have seen, a low-temperature Raman spectrum reflects the spectral variation of the product $C(\omega)g(\omega)$. It is well established that in a number of different amorphous systems $C(\omega)g(\omega)$ exhibits a behavior close to ω^4 (see, for example, Refs. 8, 13 and references therein). This is also the case in our study (Fig. 4), the frequency exponents being 3.5–3.8 for different samples. The SPM predicts instance an ω^4 dependence, and thus seems to describe correctly the universal behavior. The SPM prediction is, however, obtained within the assumptions that (1) the coupling function $C(\omega)$ does not depend on frequency, and (2) only the excess HO density of states contributes to the scattering. To our knowledge, neither of these assumptions has ever been justified experimentally. In contradiction, there is a strong evidence that at least a linear variation of $C(\omega)$ with frequency may be the general behavior, if a low-frequency Raman spectrum is assumed to reflect the *total* density of states.[9–13] A possible argument of a relatively small phonon density must be ruled out, on the basis of the heat capacity data. Indeed, the excess heat capacity around the maximum of C_p/T^3 vs T (being a measure of the maximum excess contribution in the total DVS) is comparable with the Debye contribution for the systems under investigation (see experimental points and Debye levels in Fig. 10, the other curves to be discussed below), as well as in other glasses.[13] To check whether there is any relation between the low-temperature heat capacity (which reflects the *total* DVS) and low-frequency Raman scattering (which may reflect a *part* of DVS only), we have applied the same procedure, as discussed in Ref. 13, in an attempt to fit the heat capacity from the density of states, assuming that the latter can be obtained from the low-temperature Raman spectrum with $C(\omega) \propto \omega^\alpha$. The heat capacity was calculated using the equation

$$C_p \approx C_v = 3Nk_B \int_0^{\omega_0} g(\omega) \left(\frac{\hbar\omega}{k_BT}\right)^2 \times \frac{\exp(\hbar\omega/k_BT)}{[\exp(\hbar\omega/k_BT)-1]^2}\, d\omega, \qquad (18)$$

where N is the number density, ω_0 the highest vibrational frequency, and taking the magnitude of $g(\omega)$ as the only fitting parameter. The fits (Fig. 10) can be considered as satisfactory for α in the range $0.6 \leq \alpha \leq 1.0$ for all the glasses studied (at $T = 0$ fitted curves fall to zero since we did not make any assumptions on the spectral behavior below the instrumental limit of a few cm^{-1}, just truncating the integration range). Curves calculated for $C(\omega) = \text{const}$ are also presented to make it clear that this assumption is not productive. We note that it is not possible to generate fits which are nearly as reasonable by assuming that only *excess* states contribute to Raman scattering with a smooth $C(\omega)$ (not with $C(\omega) = \text{const}$ in particular). An assumption of a steplike behavior of $C(\omega)$, changing from a constant value below the BP to another constant value above the peak,[22] is possible but seems unlikely. It hardly seems

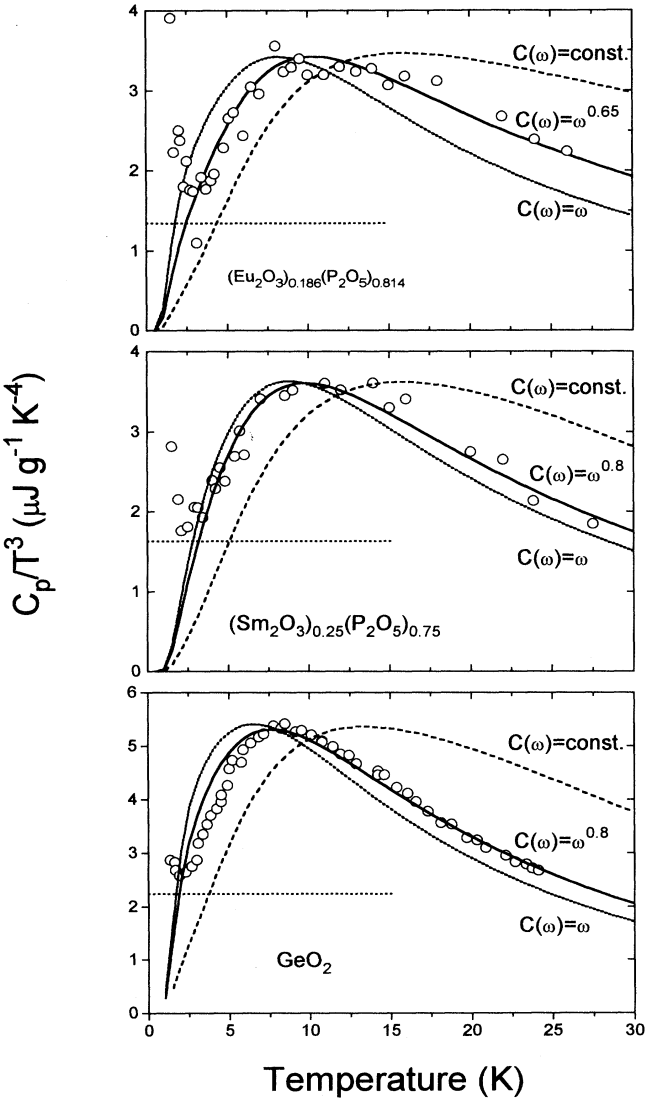

FIG. 10. Specific heat data of $(Eu_2O_3)_{0.186}(P_2O_5)_{0.814}$, $(Sm_2O_3)_{0.25}(P_2O_5)_{0.75}$ and GeO_2 glasses. Horizontal lines indicate the Debye model values calculated from the sound velocity data [Eq. (11)]. Other curves represent fit results of Eq. (18) to the data using density of states from the lowest-temperature Raman spectra and different assumptions made for $C(\omega)$, as indicated.

acceptable to explain the successful fitting of the heat capacity from Raman spectra, for a number of different glasses and under the assumption of smooth $C(\omega)$ by an accidental coincidence for a particular glass. Thus, the following conclusion may be formulated: Low-frequency Raman scattering in a number of glasses reflects the total DVS in the region of BP, with a smoothly varying coupling function which has an almost linear dependence on frequency.

Taking the difference of the approximated $g_{\text{aprx}}(\omega)$ and the Debye $g_D(\omega)$ densities of states to get an estimate of the "excess" density, one readily finds a range ($\approx$ 10–25 cm^{-1}) where an ω^4 dependence seems to describe the data reasonably (Fig. 11), and the so extracted excess $g_{\text{aprx}}(\omega)$ is then compatible with the SPM predictions. However, some precautions are needed in making this comparison of the present data with the SPM, since (1) we obtained a frequency-dependent coupling coefficient $C(\omega) \sim \omega$. This is clearly not compatible with the SPM prediction of a frequency-independent coupling coefficient, which follows from the general SPM assumption that the soft mode configuration does not depend on its eigenfrequency. (2) Our analysis suggests that Raman scattering spectrum reflects the *total* density of vibrational states. Consequently, if one separates vibrational states into the Debye and the "excess" states (which are clearly of different nature), then both must contribute to Raman scattering with *the same* (or very similar) coupling coefficients for any given frequency, a result which cannot be explained within the SPM and suggests that this separation is questionable.

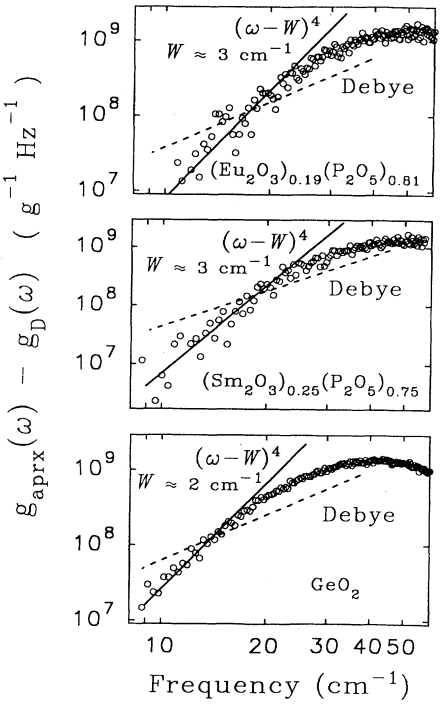

FIG. 11. Density of excess modes versus frequency as determined from the fits of Fig. 10 and subtracting respective Debye contributions calculated from the sound velocities. Solid lines represents the SPM prediction of an ω^4 proportionality and dashed lines represent a Debye densities of states.

VI. CONCLUSIONS

A study of Raman, specific heat, and ultrasonic effects in phosphate glasses which contain high concentrations of lanthanide R^{3+} ions and in glassy germanium dioxide has revealed features typical of the glassy state which can be explained in terms of low-energy excitations introduced by the topological disorder. We have shown that the temperature and frequency dependences of the relaxational part of the low-frequency Raman scattering, the QS, are in reasonable agreement with the predictions of the SPM, which explains the low-energy excitations in terms of anharmonic soft potentials schematized as double-(TLS) and single-(HO) well potentials. In particular the SPM suggests that the same relaxation mechanisms causing the plateau of acoustic attenuation and the excess contribution to the sound velocity in the temperature region below 40 K also contribute to the QS, as found in our analysis. The excess specific heat over that predicted by the Debye theory appears to be a consequence of additional vibrational states, which can be represented by a density of states characterized by a fourth-order frequency dependence which becomes linear with increasing frequency. This peculiarity seems to be in close agreement with the quasiharmonic density of soft modes predicted by the SPM. Finally the evaluation of the heat capacity through a density of states obtained by the low-frequency Raman spectrum at low temperature, where only the BP is present, leads to a nearly linear frequency dependence for the light-vibration coupling constant $C(\omega)$. This is not accounted for in the framework of the SPM, which assumes $C(\omega)$ to be frequency independent.

ACKNOWLEDGMENTS

We are grateful to Dr. H.B. Senin for the glass preparation and also to the Johnson Matthey Technology Center (Dr. A. Pratt), to DRA Maritime Division (S. Takel) for support of our programme of work on rare earth phosphate glasses, and E. Moser of Physics Department of Trento for technical support.

* On leave from Institute of Semiconductor Physics, Ukrainian Academy of Sciences, 252650 Kiev-28, Ukraine.
[1] A. Brodin, A. Fontana, L. Börjesson, G. Carini, and L. M. Torell, Phys. Rev. Lett. **73**, 2067 (1994).
[2] For a review, see *Amorphous Solids: Low-Temperature Properties*, edited by W. A. Phillips (Springer-Verlag, Berlin, 1981).
[3] S. R. Elliott, Europhys. Lett. **19**, 201 (1992).
[4] C. I. Nicholls and H. M. Rosenberg, J. Phys. C **17**, 1165 (1984).
[5] A. Fontana, F. Rocca, and M. P. Fontana, Phys. Rev. Lett. **58**, 503 (1987).
[6] S. Alexander and R. Orbach, J. Phys. (Paris) Lett. **33**, L625 (1982).
[7] R. Shuker and R. W. Gammon, Phys. Rev. Lett. **4**, 222 (1970).
[8] J. Jäckle, in *Amorphous Solids: Low-Temperature Properties* (Ref. 2), p. 135.
[9] U. Buchenau, M. Prager, N. Nüker, A. J. Dianoux, N. Ahmad, and W. A. Phillips, Phys. Rev. B **34**, 5665 (1986).
[10] A. Fontana, F. Rocca, M. P. Fontana, B. Rosi, and A. J. Dianoux, Phys. Rev. B **41**, 3778 (1990).
[11] V. K. Malinovsky, V. N. Novikov, P. P. Parshin, A. P. Sokolov, and M. G. Zemlyanov, Europhys. Lett. **11**, 43 (1990).
[12] T. Achibad, A. Boukenter, and E. Duval, J. Chem. Phys. **99**, 2046 (1993).
[13] A. P. Sokolov, A. Kisliuk, D. Quitmann, and E. Duval, Phys. Rev. B **48**, 7692 (1993).
[14] R. E. Strakna and H. T. Savage, J. Appl. Phys. **35**, 1445 (1964).
[15] G. Carini, M. Cutroni, M. Federico, and G. Galli, J. Non-Cryst. Solids **104**, 323 (1984).
[16] G. Carini, M. Cutroni, C. D'Angelo, M. Federico, G. Galli, G. Tripodo, G. A. Saunders, and W. Qingxian, J. Non-Cryst. Solids **121**, 288 (1990).
[17] J. Lorösch, M. Couzi, J. Pelous, R. Vacher, and A. Levasseur, J. Non-Cryst. Solids **69**, 1 (1984).
[18] G. Carini, M. Federico, A. Fontana, and G. A. Saunders, Phys. Rev. B **47**, 3005 (1993).
[19] V. G. Karpov, M. I. Klinger, and F. N. Ignatiev, Zh. Eksp. Teor. Fiz. **84**, 760 (1983) [Sov. Phys. JETP **57**, 439 (1983)].
[20] V. G. Karpov and D. A. Parshin, Pis'ma Zh. Eksp. Teor. Fiz. **38**, 536 (1983) [JEPT Lett. **38**, 648 (1983)].
[21] U. Buchenau, Yu. M. Galperin, V. L. Gurevich, D. A. Parshin, M. A. Ramos, and H. R. Schober, Phys. Rev. B **46**, 2798 (1992).
[22] V. L. Gurevich, D. A. Parshin, J. Pelous, and H. R. Schober, Phys. Rev. B **48**, 16 318 (1994).
[23] D. A. Parshin, Phys. Rev. B **49**, 9400 (1994).
[24] G. Carini, G. D'Angelo, M. Federico, G. A. Saunders, H. B. Senin, and G. Tripodo, Phys. Rev. B **50**, 2858 (1994).
[25] G. Carini, C. D'Angelo, G. Tripodo, and G. A. Saunders, Philos. Mag. B **71**, 539 (1995).
[26] K. E. Lipinska-Kalita, A. Fontana, A. Leonardi, G. Carini, G. D'Angelo, G. Tripodo, and G. A. Saunders, Philos. Mag. B **71**, 571 (1995).
[27] D. A. Parshin, Phys. Solid State **36**, 991 (1994).
[28] A. Fontana, G. Carini, A. Brodin, L. M. Torell, L. Borjesson, and G. A. Saunders, Philos. Mag. B **71**, 525 (1995).
[29] N. Soga, J. Appl. Phys. **40**, 3382 (1969).